ADVANCED MATERIALS

DOI: 10.1002/adma.200702522

Direct Observation of Inversion Domain Boundaries of GaN on c-Sapphire at Sub-Ångstrom Resolution**

By *Fude Liu,** *Ramon Collazo, Seiji Mita, Zlatko Sitar, Stephen J. Pennycook,* and *Gerd Duscher*

Wide-bandgap III–nitrides have seen enormous success in modern electronic, optoelectronic, and even spintronic devices.[1–5] Recently, interest has grown in manipulating the crystal polarity of GaN having a wurtzite structure, which provides a new degree of freedom for investigating III–nitrides and their novel devices.[6–10] These studies include work on the inversion domain boundaries (IDBs) of GaN, which separate adjacent domains of different polarity.[11] Ten years ago, Northrup et al. performed first-principles calculations of domain-boundary energies and proposed the structure shown in Figure 1, based on its very low energy (25 meV Å^{-2}).[11] Since then, no direct, indisputable test has been carried out to determine the exact boundary structure. At the same time, many unique properties have been observed at the IDBs.[9,12] Among these is the remarkable effect, observed by Stutzmann et al.[9] that the IDB can act as a rectifying junction when biased by two electrodes placed on adjacent Ga- and N-face regions. The boundary between two adjacent domains with different polarity has been shown to be a very efficient radiative recombination center, which may have potential application for novel light-emitting devices. Meanwhile, it was found that the rectifying behavior of the IDBs can be explained by ab initio density functional calculations,[13] assuming the IDBs have a structure as shown in Figure 1 (where a thin AlN layer is used to invert the polarity of GaN). However, the IDB structure has never been determined directly and their real structure remains unconfirmed. Here we show that we have determined directly the IDB structure, including the determination of GaN polarity, by aberration-corrected scanning transmission electron microscopy (STEM) at sub-Ångstrom resolution (ca. 0.8 Å). We propose also an improved method to make such an IDB structure intentionally, which may avoid the problems with conventional approaches.

As shown in Figure 1, the stable wurtzite structure of III–nitrides has a polar axis parallel to the *c*-direction of the crystal lattice. The *c*-direction is usually defined along the direction in which the III atoms of the III–nitride bilayers forming the crystal are facing the sample surface. Owing to the strong charge transfer between the very electronegative N atoms and the less electronegative Ga atoms and the deviation of the real *c*/*a* ratio (1.626) from the ideal *c*/*a* ratio ($\sqrt{8/3} \approx 1.633$; in the specific case of GaN; *c* and *a* are the lattice constants), a macroscopic spontaneous polarization *P* exists in GaN.[10,14] This spontaneous polarization *P* (and the piezoelectric polarization in the case of III–nitride crystals grown on a heterosubstrate) corresponds to a large internal electric field *E* with opposite direction. Because of these physical principles behind and the related unique properties, it is particularly interesting to explore the possibility of the growth of lateral-polarity heterostructures as mentioned above. Therefore, there is strong motivation to determine unambiguously the IDB structure.

The experimental challenges are the lack of required lateral spatial resolution and/or the lack of ability for discriminating the low-*Z* atoms (N, in this case) from the high-*Z* atoms (Ga, in this case), where *Z* is the atomic number. As seen in Figure 1 (or Fig. 2a), assuming this model is correct, the smallest projected spacing between Ga and N columns is ca. 1.1 Å in the $[\bar{2}110]$ projection. In addition, the Ga lattice (or the N lattice) on the right side of the IDB shifts up (or down) by 0.64 Å compared with the Ga lattice (or the N lattice) on the left side. Therefore, a very small electron probe is required for discrimination. Conventional high-resolution transmission electron microscopy (HRTEM) is not direct imaging and requires extensive postprocessing of the focal series of image data, which increases the risk of introducing image artifacts.[15] Figure 3 shows HRTEM images taken in the $[\bar{2}110]$ projection at a GaN IDB contained intrinsically in the GaN film grown directly on *c*-sapphire. We can see that the IDB originates at the interface with the sapphire substrate, is straight, and lies on the $(01\bar{1}0)$ plane. The two sides of the IDB have different phase contrasts, which may indicate that the two sides have different polarity. However, we do not know with certainty the coordinates around the IDB or the polarity on either side of the IDB.

[*] Dr.F. Liu,[+] Dr.R. Collazo, S. Mita, Prof.Z. Sitar, Prof. G. Duscher
Department of Materials Science and Engineering
North Carolina State University
Raleigh, NC 27606 (USA)
E-mail: fude_liu@nrel.gov
Prof.S. J. Pennycook, Prof. G. Duscher
Materials Science and Technology Division
Oak Ridge National Laboratory
Oak Ridge, TN 37831 (USA)
[+] Present address: MailStop 3215, National Center for Photovoltaics, National Renewable Energy Laboratory, Golden, CO 80401, USA.

[**] This work has been funded by the Office of Naval Research under contract number N00014-01-1-0716, with Dr. Colin Wood, project monitor, and by the Division of Materials Science and Engineering (SJP), U.S. Department of Energy.

WILEY InterScience DISCOVER SOMETHING GREAT
© 2008 WILEY-VCH Verlag GmbH & Co. KGaA, Weinheim

Recent developments in aberration-corrected STEM allow the direct imaging of a crystal lattice.[16] In a STEM, an electron beam is focused into a tiny probe, which is scanned over the sample in a raster. The images are recorded in annular dark-field (ADF) image mode, where only large-angle, Rutherford-scattered electrons are collected with an ADF detector, which causes its image intensity to be approximately proportional to Z^2.[17] ADF-STEM imaging has obvious advantages over traditional phase-contrast HRTEM imaging, that is, it is relatively insensitive to focus conditions and specimen thickness, and its image can be interpreted directly in terms of atomic coordinates.

The same GaN IDB shown in Figure 3 was imaged with high-angle (HA)ADF-STEM imaging. Figure 2b shows a HAADF-STEM image of the IDB, recorded in the $[\bar{2}110]$ projection, using a VG Microscopes HB603U 300-kV STEM fitted with a Nion aberration corrector, giving an expected probe size in the range of 0.8 Å.[16] First, note that the Ga lattice shift Δd is measured to be ca. 0.6 Å, which is consistent with the IDB model in Figure 2a. Also note that Figure 2b is dominated by the strong scattering of Ga columns. To determine the N column positions and then the polarity of the GaN lattice, one HAADF-STEM image was acquired from a very thin (<10 nm) region on the right side of the IDB, as shown in Figure 2c. In this figure, the N columns are seen as elongations of the Ga column images alternately pointing diagonally left and right. The same image is fitted with both a Ga-face lattice and an N-face lattice. The former one fits the experimentally obtained image well, whereas the latter does not fit it at all. Given the 0.6 Å shift of the left side of the IDB, it must therefore have the N-face polarity, although it is unclear in the image owing to, most likely, even a very small specimen tilt. Direct determination of a crystal lattice polarity was realized recently on AlN, where the weaker scattering of Al atoms (which have a lower Z, 13) makes it easier to see the N columns.[18] Although the much stronger scattering of Ga atoms (which have a much higher Z, 31) makes it difficult to determine GaN polarity directly, we demonstrate here that this is possible with an aberration-corrected STEM at the resolution of ca. 0.8 Å. This result is consistent with our convergent-beam electron diffraction (CBED) results, which show that the two sides of the IDB have opposite polarity.

To determine the polarity of GaN with CBED, the zone axis $[0\bar{1}10]$ is usually chosen because of the clearer CBED pattern features, compared with the patterns obtained on zone axis $[\bar{2}110]$, although ADF-STEM imaging and HRTEM imaging of the GaN lattice structure are often obtained on zone axis $[\bar{2}110]$. Therefore, one more TEM specimen was prepared, cutting along the $\{0\bar{1}10\}$ planes, instead of along the $\{\bar{2}110\}$ planes. Figure 4a shows a low-angle (LA) ADF-STEM image of the GaN film in the $[0\bar{1}10]$ projection. A typical straight, dark ca. 58 nm stripe was observed in the GaN film, which corresponds to a 30° inclined IDB in the $[0\bar{1}10]$ projection, as confirmed by the convergent-beam electron diffraction (CBED) results. Actually, the width of the stripe changed when the specimen was tilted in the {0001} planes. Note that the

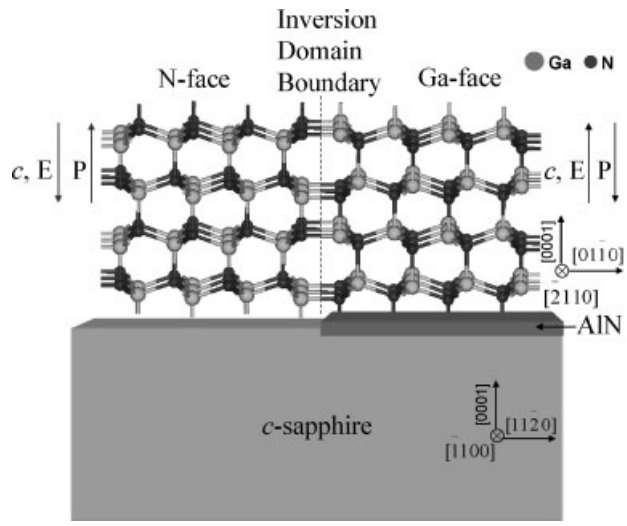

Figure 1. Schematic view of the widely cited GaN IDB structure on a sapphire substrate (not drawn to scale). A thin AlN layer (>5 nm) is often applied to invert the polarity of GaN. On the left side, the GaN lattice has N-face polarity, the crystallographic *c*-axis and the internal electric field *E* point toward the interface with the substrate, and the macroscopic polarization *P* points toward the surface. On the right side, the directions are inverted.

IDB shown here is still on the $(0\bar{1}10)$ plane, just as the one shown in Figures 1–3. The two sides of the boundary have opposite polarity, as seen from the different contrasts in the 0002 and $000\bar{2}$ disks owing to the strong dynamical effect of electron diffraction (Fig. 4b); this confirms that this boundary is indeed an IDB. Also, the detected regions have a thickness of ca. 100 nm by matching the experimentally obtained CBED patterns with the simulated one, using the Bloch-wave approach (Fig. 4c). The atomic model of the IDB is shown in Figure 4d, which corresponds well with the experimental results. The CBED results indicate that the IDBs studied in this work prefer to form on the $\{0\bar{1}10\}$ planes and are straight (which is good for device applications); this further confirms our HAADF-STEM imaging results at sub-Ångstrom resolution.

Much effort has been put in the growth of lateral-polarity heterostructures with IDBs.[9,19] The basic steps usually involve patterning a low-temperature AlN layer coated on nitrided sapphire by photolithography and subsequent overgrowth of GaN on the whole surface. However, we found that the sharp IDB shown in Figure 1 could not be obtained with this approach (details will be published elsewhere). This may be related to (i) the difficulty to align the end edge of the AlN layer along the $[\bar{2}110]$ direction, and (ii) the atomic roughness of the end edge because of the limited resolution of photolithography and chemical (or reactive ion) etching. To avoid these possible problems with this approach, we propose an improved method that may help us actually make such an IDB structure intentionally. As shown in Figure 5, a narrow SiO_2 (or SiN) mask is applied to cover the end edge of the AlN layer. This mask not only covers the rough end edge, but also

 © 2008 WILEY-VCH Verlag GmbH & Co. KGaA, Weinheim

ADVANCED MATERIALS

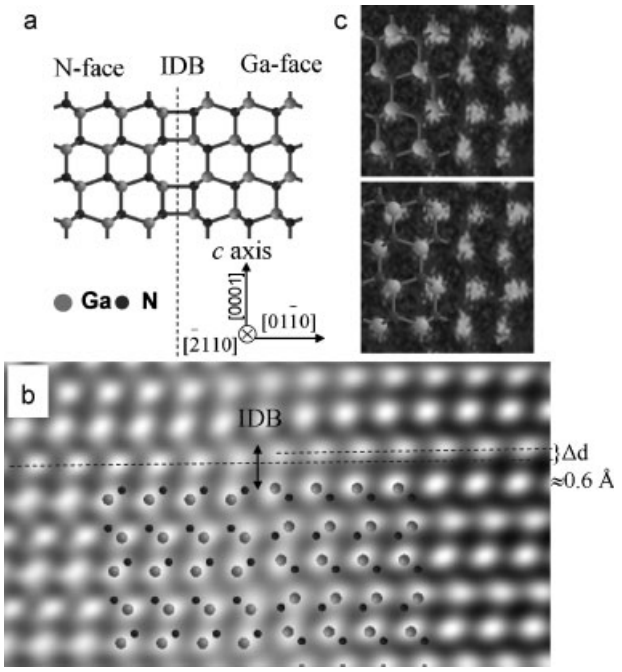

Figure 2. Theoretical and experimental IDB structure and the polarity of GaN. a) The widely accepted GaN IDB model. The [0001] direction (or $+c$ axis) is defined along the Ga-face lattice polarity, whereas the [000$\bar{1}$] direction (or $-c$ axis) is along the N-face lattice polarity. b) High-angle annular dark-field (HAADF)-STEM image of the same GaN IDB as the one shown in Fig. 3 in the [$\bar{2}$110] projection. The theoretical IDB structure fits the experimentally obtained structure well. The image has been low-pass-filtered to reduce the noise. c) Two opposite-polarity lattices are used to fit the same HAADF-STEM image acquired from a very thin region on the right side of the IDB. The Ga-face lattice fits the lattice image, whereas the N-face lattice does not. It can indicate the polarity of GaN directly.

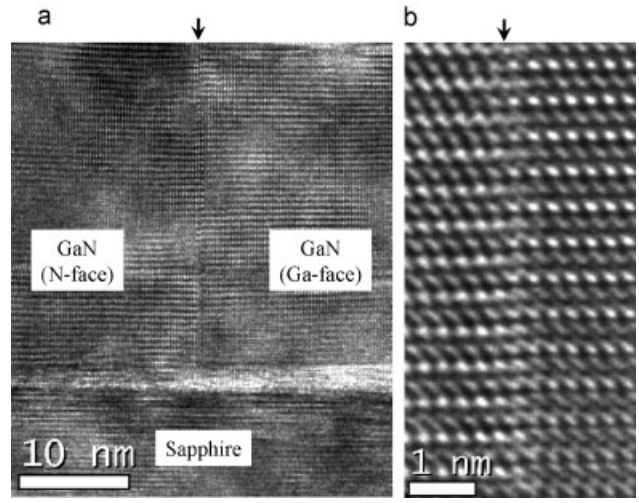

Figure 3. Phase-contrast HRTEM images in the [$\bar{2}$110] projection. a) Low-magnification HRTEM image taken at a straight GaN IDB contained intrinsically in the GaN film grown directly on *c*-sapphire. The IDB is indicated by the arrow. The polarity is determined directly, as shown in Fig. 2c. b) High-magnification HRTEM taken at the same IDB. The IDB is indicated by the arrow. The two sides of the IDB have different phase contrasts, which may indicate that the two sides have different polarity.

increases the tolerance of the AlN end edge misalignment along the [$\bar{2}$110] direction. The subsequent overgrowth of GaN on the whole surface causes the lateral epitaxial overgrowth of GaN layer on the SiO_2 (or SiN) mask; a sharp and straight IDB (which is good for device applications) is expected when the two domains with opposite polarity meet. It needs to be pointed out that the real situations may be much more complicated than the simple picture presented here. However, more research work towards this promising method of making IDBs intentionally should be worthwhile.

The present findings therefore clearly show, for the first time, that the widely cited IDB theoretical structure can indeed exist in reality. This kind of IDB structure has its origin in the very low boundary-wall energy on the {0$\bar{1}$10} planes (20–25 meV Å^{-2}) as deduced from first-principles calculations (which we repeated, obtaining similar results).[11,13] Such a structural determination will enable a new understanding of the atomic-scale origins of the unique electronic properties of a GaN IDB and its devices. It increases

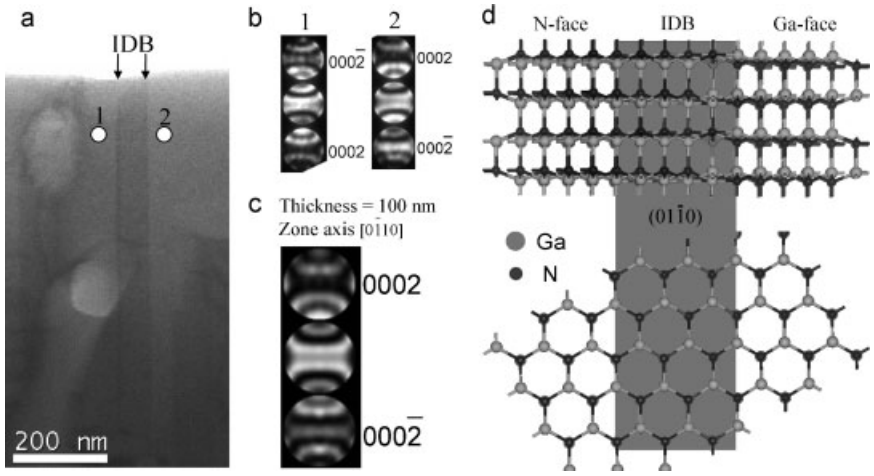

Figure 4. Convergent-beam electron diffraction (CBED) results. a) LAADF-STEM image of the GaN film in the [0$\bar{1}$10] projection. The IDB is indicated by the arrows as a dark stripe. "1" and "2" represent two positions where the CBED patterns were acquired. b) Two CBED patterns show the opposite polarity of position "1" and "2." c) Simulated CBED pattern. The measured region thickness is ca. 100 nm, as indicated by the match of the experimentally obtained CBED patterns and the simulated pattern. d) Atomic model of the IDB, including the cross-sectional view (top) and the top-down view (bottom). The inclined IDB (0$\bar{1}$10) plane is shown in grey.

© 2008 WILEY-VCH Verlag GmbH & Co. KGaA, Weinheim

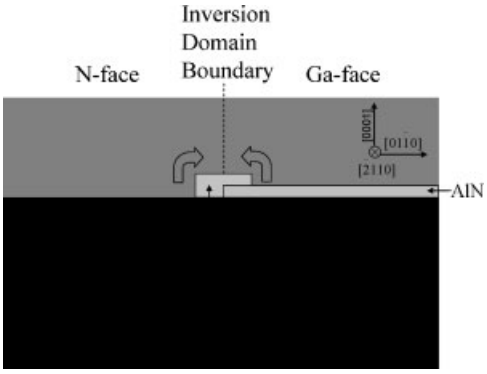

Figure 5. Schematic of an improved growth method of lateral-polarity heterostructures. The block arrows indicate the lateral epitaxial overgrowth of GaN layer on SiO_2 (or SiN) mask.

our confidence that we may actually make such an IDB structure intentionally. We believe that the ability to determine directly the IDB structure, including the determination of GaN polarity, with an aberration-corrected STEM at sub-Ångstrom resolution, will also spur major interest among the III–nitride community in engineering lattice polarity as a new degree of freedom for investigating III–nitrides and their devices (and other polar materials such as ZnO[20]).

Experimental

A ca. 1 μm thick GaN film was grown directly on *c*-sapphire at a temperature of 1030 °C with a V/III ratio of around 100 by low-pressure metal–organic vapor phase epitaxy (MOVPE) process. N_2 was used as dilution and carrier gas throughout the growth process. The details of the growth process have been presented elsewhere [21]. The transmission electron microscopy (TEM) specimens were prepared by the standard mechanical grinding and ion-milling method. The final step of specimen preparation was done at low voltage (2.0–0.5 kV) and high milling angle (15 °–17 °) with a Fischione ion mill (Model 1010) to minimize the artifacts introduced during specimen preparation. ADF-STEM images were taken with a VG Microscopes HB603U 300-kV STEM fitted with a Nion aberration corrector at Oak Ridge National Laboratory, giving an expected probe size in the range of 0.8 Å. The ADF detector collected electrons scattered by the sample to angles greater than the detector inner radius of 70 mrad. The images were low-pass-filtered to reduce the noise by using Gatan DigitalMicrograph software. The CBED patterns were acquired with a JEOL2010F TEM/STEM operated in STEM mode at 200 kV at North Carolina State University. The simulated CBED patterns were done with Electron Microscopy Software (Java version), using the Bloch-wave approach. The traditional phase-contrast HRTEM images were also taken with this microscope.

Received: October 7, 2007
Revised: December 24, 2007
Published online: April 22, 2008

[1] Y. Taniyasu, M. Kasu, T. Makimoto, *Nature* **2006**, *441*, 325.
[2] L. F. Eastman, U. K. Mishra, *IEEE Spectrum* **2002**, *39*, 28.
[3] S. A. Wolf, D. D. Awschalom, R. A. Buhrman, J. M. Daughton, S. Molnár, M. L. Roukes, A. Y. Chtchelkanova, D. M. Treger, *Science* **2001**, *294*, 1448.
[4] M. S. Shur, R. F. Davis, *GaN-Based Materials and Devices — Growth, Fabrication, Characterization and Performance*, World Scientific, Singapore **2004**.
[5] F. Ponce, T. D. Moustakas, I. Akasaki, B. Monemar, *III-V Nitrides*, Materials Research Society, Pittsburgh, PA **1997**.
[6] E. S. Hellman, *MRS Internet J. Nitride Semicond. Res.* **1998**, *3*, 11.
[7] R. Dimitrov, M. Murphy, J. Smart, W. Schaff, J. R. Shealy, L. F. Eastman, O. Ambacher, M. Stutzmann, *J. Appl. Phys.* **2000**, *87*, 3375.
[8] G. Koley, M. G. Spencer, *Appl. Phys. Lett.* **2005**, *86*, 042107.
[9] M. Stutzmann, O. Ambacher, M. Eickhoff, U. Karrer, A. L. Pimenta, R. Neuberger, J. Schalwig, R. Dimitrov, P. J. Schuck, R. D. Grober, *Phys. Status Solidi B* **2001**, *228*, 505.
[10] F. Bernardini, V. Fiorentini, *Phys. Rev. B* **1997**, *56*, 10024.
[11] J. E. Northrup, J. Neugebauer, L. T. Romano, *Phys. Rev. Lett.* **1996**, *77*, 103.
[12] P. J. Schuck, M. D. Mason, R. D. Grober, O. Ambacher, A. P. Lima, C. Miskys, R. Dimitrov, M. Stutzmann, *Appl. Phys. Lett.* **2001**, *79*, 952.
[13] V. Fiorentini, *Appl. Phys. Lett.* **2003**, *82*, 1182.
[14] A. Zoroddu, F. Bernardini, P. Ruggerone, *Phys. Rev. B* **2001**, *64*, 045208.
[15] C. Iwamoto, X. Q. Shen, H. Okumura, H. Matuhata, Y. Ikuhara, *Appl. Phys. Lett.* **2001**, *79*, 3941.
[16] P. D. Nellist, M. F. Chisholm, N. Dellby, O. L. Krivanek, M. F. Murfitt, Z. S. Szilagyi, A. R. Lupini, A. Borisevich, W. H. Sides, Jr., S. J. Pennycook, *Science* **2004**, *305*, 1741.
[17] R. F. Egerton, *Physical Principles of Electron Microscopy*, Spinger, New York **2005**.
[18] K. A. Mkhoyan, P. E. Batson, J. Cha, W. J. Schaff, J. Silcox, *Science* **2006**, *312*, 1354.
[19] A. Aleksov, R. Collazo, S. Mita, R. Schlesser, Z. Sitar, *Appl. Phys. Lett.* **2006**, *89*, 052117.
[20] P. X. Gao, Y. Ding, W. Mai, W. L. Hughes, C. Lao, Z. L. Wang, *Science* **2005**, *309*, 1700.
[21] R. Collazo, S. Mita, A. Aleksov, R. Schlesser, Z. Sitar, *J. Cryst. Growth* **2006**, *287*, 586.

© 2008 WILEY-VCH Verlag GmbH & Co. KGaA, Weinheim